



Novel 2,6-disubstituted-3-(2H)-pyridazones as Cholinesterase Inhibitors: *In vitro* Enzyme Inhibition and *In silico* Molecular Modelling and Dynamic Studies

Azime Berna Özçelik^{1*}, Hasan Erkan Rüzgar¹, Fatma Sezer Şenol Deniz², İlkay Orhan Erdoğan²,
Mehmet Abdullah Alagöz³, Zeynep Özdemir³

¹Gazi University, Faculty of Pharmacy, Department of Pharmaceutical Chemistry, 06330 Ankara, Turkey

²Gazi University, Faculty of Pharmacy, Department of Pharmacognosy, 06330 Ankara, Turkey

³Inonu University, Faculty of Pharmacy, Department of Pharmaceutical Chemistry, 44280

Malatya, Turkey

Article info:

Received: 25.05.2022

Accepted: 21.06.2022

Keywords:

Alzheimer,
AChE,
BChE,
Pyridazinone,
Molecular docking

Abstract

The approach proposed as the cholinergic hypothesis for Alzheimer's Disease contributed significantly to the explanation of cognitive decline observed in the elderly and Alzheimer's patients due to dysfunction of neurons containing acetylcholine in the brain. To date, this notion has formed the basis of most of the treatment strategies and drug development approaches for Alzheimer Disease. Within the scope of this study, in which the synthesis and biological evaluation of pyridazinones, which are designed for multi-enzyme targets and expected to act as AChE and BChE inhibitors, were performed, 12 new compounds were synthesized, their *in vitro* enzyme inhibitor activities were evaluated and molecular modeling studies were carried out. While the compounds did not show significant AChE inhibition, they showed a high degree of BChE inhibition. D2e was determined as the most potent BChE inhibitor and molecular modeling and molecular dynamics simulation studies were also carried out for D2e and tacrine. The obtained results suggest that new pyridazinone derivatives can act as BChE inhibitory agents. Although the synthesized compounds are less effective than the reference drugs, it has been concluded that it is possible to reach the precursor compounds as a result of suitable modifications.

1. Introduction

Alzheimer's disease (AD), which starts with the deterioration of the patient's ability to perform daily activities in the early stages, manifests itself with cognitive dysfunction and different neuropsychiatric symptoms in the later stages, and this irreversible process results in death (Özdemir et al., 2019). Although the pathophysiology of AD is not fully known yet, it is thought to be caused by the loss of brain cells with an undetermined cause, and three main hypotheses (cholinergic hypothesis, amyloid hypothesis and tau hypothesis) have been proposed regarding the formation of the disease (Özdemir et al., 2019). According to the cholinergic hypothesis, which is the oldest of the hypotheses put forward, it is thought that AD occurs due to the decrease of acetylcholine, an important neurotransmitter in the development of the disease. Degeneration of cholinergic neurons in the basal forebrain in Alzheimer's patients; there is a significant decrease in cholinergic receptors and choline acetyl transferase (ChAT) levels in the cerebral cortex. Although many of the previous treatment approaches are based on

this hypothesis, clinical studies have revealed that treatment strategies to increase acetylcholine levels provide symptomatic relief (Figure 1) (Hampel et al., 2018; Anand & Singh, 2013). Recent studies on the cholinergic hypothesis suggest that the use of cholinesterase inhibitors may affect the occurrence of amyloid fibrillation (Sameem et al., 2018).

Acetylcholinesterase and butyrylcholinesterase enzymes in the serine hydrolase enzyme group are generally known as cholinesterases. Although cholinesterase enzymes are encoded in different chromosomes, the amino acid sequences of both enzymes are 65% similar to each other (Figure 2) (Çeçen et al., 2020). It is known that AChE and BChE are responsible for 80% and 20%, respectively, of cholinesterase activity in the human brain. The levels of AChE and BChE enzymes vary during the development of the nervous system. The BChE ratio decreases with the progression of this developmental process. The regions of AChE and BChE enzymes in cholinergic neurons also differ.

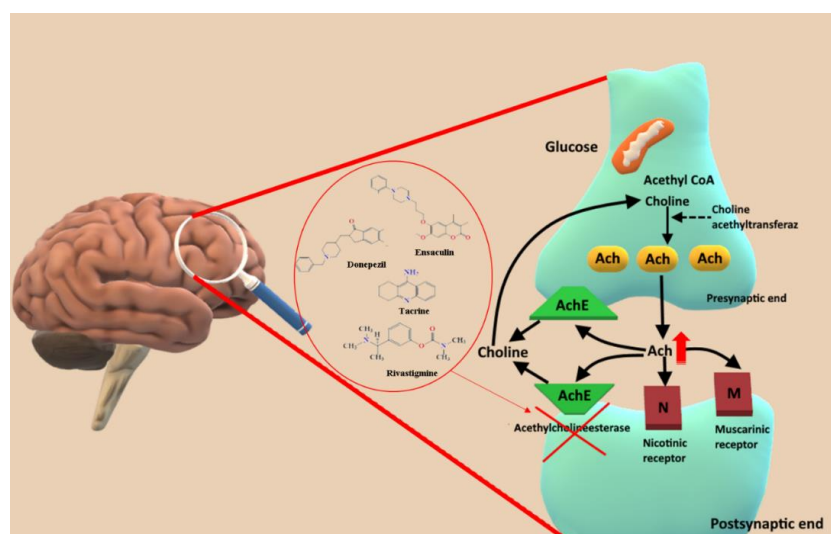


Figure 1: Cholinergic hypothesis

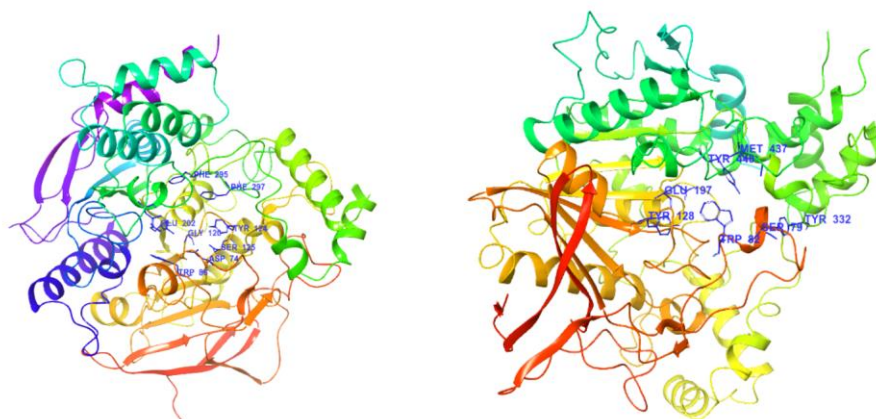


Figure 2: 3D Structures and active sites of AChE and BChE

While AChE and BChE are located in the neuron body and dendrites, AChE is located in axons (Dvir et al., 2010). It has been reported that AChE and BChE act together in the anatomical development of the nervous system and in cholinergic transmission (Chatonnet, & Lockridge, 1989).

The pyridazine core represents a versatile framework for developing new pharmacologically active compounds. The heterocyclic nitrogen structure is heavily involved in the structure of compounds with broad biological activity and can also be used to bind other pharmacophoric groups (Sabt et al,2020; Ahmed et al,2020; Roth et al,2015; Costas-Lago et al,2017; Kilic et al,2018). Numerous pharmacological activity studies have been carried out on the compounds with the 3(2*H*)-pyridazinone structure, and in the studies carried out, the compounds carrying this skeleton. It has been reported that they have many biological activities such as analgesic, anti-inflammatory, antihypertensive, cardiotoxic, antiplatelet, antibacterial, antifungal, antitumoral and herbicide activities. In addition, there are a number of publications reporting simple pyridazine or pyridazin-3(2*H*)-one derivatives as ligands of several

targets involved in different neurological and psychiatric disorders including PD and AD, such as GABAA receptor, excitatory amino acid transporter 2 (EAAT2), γ -secretase or formyl peptide receptors (FPRs) (Özdemir et al., 2019; Banerjee, 2011; Tan et al, 2012; Ciftci et al., 2018; Rathish et al., 2009). However, there are few studies on pyridazinone derivatives acting as selective AChE and BChE inhibitors (Çeçen et al., 2020; Yamali et al., 2015; Utku et al., 2011; Özdemir et al., 2017; Özçelik et al., 2019; Bozbey et al., 2020).

In order to develop new choline esterase inhibitor compounds, 12 new 2,6-disubstituted-3-(2*H*)-pyridazine derivatives were designed and synthesized. There are choline binding site and peripheral anionic region (PAS) responsible for the activity in the structure of the cholinesterase enzyme. It is aimed that the substituted phenyl ring in the structure of these derivatives interacts with the choline binding site, and the tertiary nitrogen interacts with PAS. In addition, structural activity studies were carried out by adding different substituents (methoxy, chloro, bromo and fluoro) to the phenyl ring. Ellman's method was used to

evaluate the cholinesterase inhibitory activities of these synthesized derivatives.

The availability of 3D structures of molecular drug targets and advances in computational approaches and bioinformatics speed up the application of molecular modeling in discovery. For this purpose, binding modes of the synthesized compounds to AChE and BChE enzymes as well as the key interactions in their active sites were determined via molecular docking simulations. Using molecular docking approach, we tried to understand binding interactions of our derivatives in the active site of both enzymes. Molecular dynamics simulation (MDS) studies were also done for most active compound, D2a to determine the interaction between this compound and BChE. It has many advantages over docking because docking gives only binding free energy of ligand with the receptor. Additionally, we can predict the actual interaction of the ligand with receptors through MDS at the atomic level.

2. Materials and Methods

2.1. Chemistry

All the chemicals were obtained from the commercial suppliers. 6-(4-substitutedphenyl)pyridazin-3(2*H*)-one derivatives **A**_{1,2}, ethyl 6-(4-substitutedphenyl)pyridazin-3(2*H*)-one-2-yl propionate derivatives **B**_{1,2} and 6-(4-substitutedphenyl)pyridazin-3(2*H*)-one-2-yl propiohydrazide derivatives **C**_{1,2} were synthesized according to literature methods (Bozbey et al., 2020). All title compounds **D**_{1a-1f}, **D**_{2a-2f} were synthesized (Özçelik et al., 2019; Bozbey et al., 2020). Melting points (mp) were recorded on a Electrothermal 9200 capillary melting point apparatus and uncorrected.

The structures were elucidated by evaluation of MASS and NMR spectra. ¹H-NMR (400 MHz) and ¹³C-NMR (300 MHz) spectra were recorded in CDCl₃ and DMSO-d₆ with Bruker Avance Neo 500 Ultrashield™ (Germany) NMR spectrometer and the chemical shifts are reported as δ (ppm) values using tetramethylsilane as internal reference. The splitting patterns were noted as s (singlet), d (doublet), t (triplet), q (quartet), m (multiplet), and dd (doublet of doublet). The mass spectra (HRMS) of the compounds were recorded on Waters Acquity Ultra Performance Liquid Chromatography Micromass and combined with LCT Premier™ XE UPLC/MS TOFF spectrophotometer (Waters Corp, Milford, USA) by ESI+ and ESI- techniques.

2.1.1. General experimental procedure for synthesis

2-(3-(4-chloro/bromophenyl)-6-oxopyridazin-1(6*H*)-yl)-*N'*-(1-(substitutedphenyl)ethylidene)acetohydrazide (**D1a-D1d**, **D2a-D2d**) derivatives were synthesized according to Figure 3.

6-(substitutedphenyl)-3(2*H*)-pyridazinone-2-yl-acetohydrazide (**C1-C2**) derivatives were synthesized according to literature (Özçelik et al., 2019; Bozbey et al., 2020). The physical and spectral properties of the starting compounds were in accordance with the literature (Bozbey et al., 2020).

2-(3-(4-chloro/bromophenyl)-6-oxopyridazin-1(6*H*)-yl)-*N'*-(1-(substitutedphenyl)ethylidene)acetohydrazide

Mixture of the appropriate 6-(substitutedphenyl)-3(2*H*)-pyridazinone-2-yl-acetohydrazide (**C1-C2**) derivatives (0.01 mol) and substituted acetophenone

(0.01 mol) in methanol (10 ml) containing two drops of acetic acid was heated under reflux for 6 h. The reaction mixture was cool. The formed precipitate was filtered, dried, and crystallized from methanol/water. All of the title compounds were reported for the first time in this study.

2.2. Anticholinesterase Activity

The *in vitro* inhibition of AChE and BChE for the new synthesized title compounds was determined by the method of Ellman et al. (1961) using galantamine (CAS 357-70-0) as reference. Electric eel AChE (Type-VI-S, EC 3.1.1.7, Sigma, St. Louis, MO, USA) and horse serum BChE (EC 3.1.1.8, Sigma) were employed as the enzyme sources, while acetylthiocholine iodide and butyrylthiocholine chloride (Sigma) as substrates and 5,5'-dithio-bis(2-nitrobenzoic)acid (DTNB) were also used in the anticholinesterase activity determination. All reagents and conditions were the same as described recently (Utku et al., 2011; Orhan et al., 2008).

2.3. Molecular Docking / MD Simulations Studies

All molecular modeling studies were performed using Schrodinger (Maestro 12.8). The structures of the ligands were drawn with the 2D Sketcher module of the Maestro program. OPLS_2005 force field parameters were applied for optimization. After appropriate tautomer and ionization conditions of ligand models were determined by LigPrep (Schrodinger, LLC, NY) software, ligands were prepared for modeling. For anticholinesterase studies, crystal structures of AChE and BChE proteins, respectively, 4EY7 and 4BDS pdb coded

structures were downloaded from the RCSB Protein Data Bank (www.rcsb.org) (Türkeş et al., 2021; Özten et al., 2021). These crystal structures were prepared using Maestro's protein preparation wizard panel. Unwanted solvent molecules, ligands in crystal structures were deleted and hydrogens were added with Prime, Impact, Epik and Propka (Schrodinger, LLC, NY) software. The active sites of the target proteins were determined and grid maps were created for each protein. Ligands were docked to these maps 100 times in standard precision mode with Glide (Maestro, LLC, NY) software (Alagöz et al., 2019).

The molecular dynamics (MD) simulations of the compounds were made using the Desmond software of the Maestro 12.8 (Schrodinger, NewYork) program. Protein ligand complexes were placed in a 10 Å thick cubic box. TIP3P water model was used in the simulation box. The system was neutralized using Na⁺ and Cl⁻ ions. The concentration of the system was adjusted with 0.15M NaCl solution. Desmond's default relaxation protocol has been applied to the simulation system (Özten et al., 2021).

3. Results

3.1. Synthesis

All of the N'-(substituted- α -methylbenzylidene)-2-(3-(4-substituephenyl)-6-oxopyridazin-1(6H)-yl)acetohydrazide **D**_{1a-1f}, **D**_{2a-2f} derivatives were reported first time in this study. New N'-(substituted- α -methylbenzylidene)-2-(3-(4-substituephenyl)-6-oxopyridazin-1(6H)-yl)acetohydrazide derivatives were synthesized according to Scheme 1.

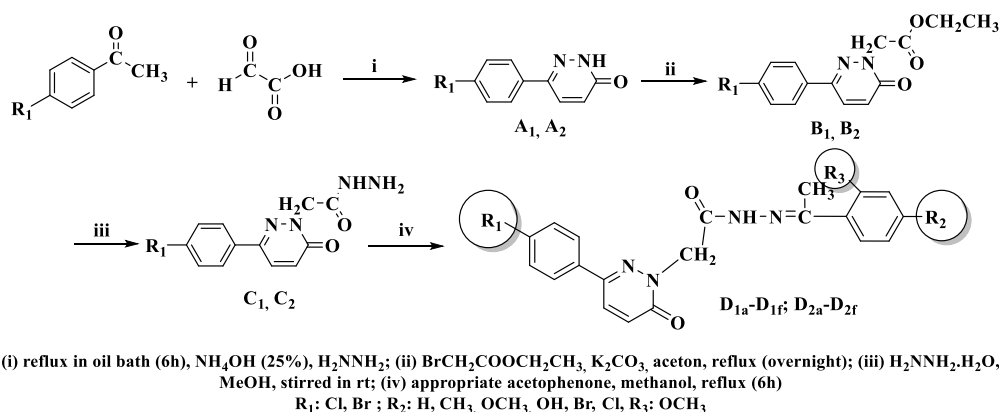


Figure 3. Synthesis of the A1-2, B1-2, C1-2 and D1a-1f, D2a-2f compounds

The reaction yields of the compounds range approximately from 40 to 61%. The physical and spectral properties of starting compounds were accordance with the literature (Bozbey et al. 2020). All spectral data of the compounds were in accordance with the assigned structures as shown following. The structures, melting points and yields of the synthesized compounds are given in Table 1.

All of the title compounds (**D1a-1f**, **D2a-2f**) were reported for the first time in this study.

2-(3-(4-chlorophenyl)-6-oxopyridazin-1(6H)-yl)-N'-(1-phenylethylidene)acetohydrazide (D1a)

137.64 (1C; pyridazinone C⁵), 143.61 (1C; pyridazinone C⁶), 148.97 (1C; pyridazinone C⁴), 159.93 (1C; N-CH₂-C=O), 168.91 (1C; pyridazinone C³). $\text{C}_{20}\text{H}_{17}\text{N}_4\text{O}_2\text{Cl}$ MS (ESI+) calculated: 381.1118, Found: m/e 381.1107 (M+H; % 100.0).

2-(3-(4-chlorophenyl)-6-oxopyridazin-1(6H)-yl)-N'-(1-(p-tolyl)ethylidene)acetohydrazide (D1b)

$^1\text{H-NMR}$ (DMSO- d_6 , 300 MHz), δ 2.4 (3H, s, methyl protons), 2.3 (3H, s, methyl protons), 5.3 and 5.002 (2H; s; -N-CH₂-C=O), 7.1 (d; 1H; 9.6 Hz;

$^1\text{H-NMR}$ (DMSO- d_6 , 300 MHz), δ 2.3 (3H, s, methyl protons), 5.3 and 5.005 (2H; s; -N-CH₂-C=O), 7.1 (1H; d; 9.6 Hz; pyridazinone H⁴), 7.3 (3H; m; phenyl protons), 7.5 (d, 2H, J = 7.6 Hz, phenyl protons) ve 7.8 (2H; m; phenyl protons), 7.9 (d, 2H, J = 7.6 Hz, phenyl protons), 8.1 ppm (1H; d; J = 9.6 Hz; pyridazinone H⁵), 10.983 (1H; s; -NH-N). $^{13}\text{C-NMR}$ (DMSO- d_6 , 75 MHz), δ 12.91 (1C; -CH₃), 54.26 (1C; -N-CH₂-C=O), 126.22 (1C; =CH), 127.27 (1C; phenyl C¹), 128.47 (2C; phenyl C^{2,6}), 129.13 (2C; phenyl C^{3,5}), 129.58 (1C; phenyl C⁴), 130.20 (1C; 4-chlorophenyl C¹), 130.35 (2C; 4-chlorophenyl C^{2,6}), 133.11 (2C; 4-chlorophenyl C^{3,5}), 135.61 (1C; 4-chlorophenyl C⁴),

pyridazinone H⁴), 7.2 (d, 2H, J = 8.4 Hz, phenyl protons), 7.5 (d, 2H, J = 8.8 Hz, phenyl protons), 7.7 (d, 2H, J = 8.4 Hz, phenyl protons), 7.9 (d, 2H, J = 8.8 Hz, phenyl protons), 8.1 ppm (1H; d; J = 9.6 Hz; pyridazinone H⁵), 10.983 (1H; s; -NH-N). $^{13}\text{C-NMR}$ (DMSO- d_6 , 75 MHz), $^{13}\text{C-NMR}$ (DMSO- d_6 , 300 MHz), δ 12.69 (1C; -CH₃), 21.30 (1C; -CH₃), 54.27 (1C; -N-CH₂-C=O), 126.14 (1C; =CH), 127.29 (1C; (4-methylphenyl C¹), 129.11 (1C; 4-methylphenyl C⁴), 129.20 (2C; 4-methylphenyl C^{2,6}), 130.23 (2C; 2-methylphenyl C^{3,5}), 130.23 (1C; 4-chlorophenyl C¹), 130.37 (2C; 4-chlorophenyl C^{2,3,5,6}), 133.14 (1C;

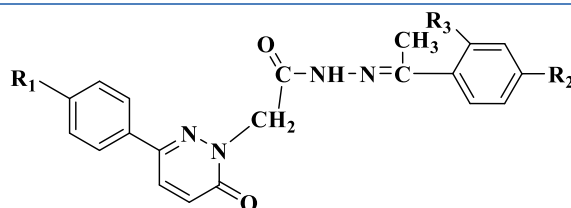
4-chlorophenyl C⁴), 134.77 (1C; pyridazinone C⁵), 139.83 (1C; pyridazinone C⁶), 148.69 (1C; pyridazinone C⁴), 159.92 (1C; N-CH₂-C=O), 168.52 (1C; pyridazinone C³). C₂₁H₂₀N₄O₂Cl MS (ESI+) calculated: 395.1275 Found: *m/e* 395.1281 (M+H; % 100.0).

2-(3-(4-chlorophenyl)-6-oxopyridazin-1(6H)-yl)-N'-(1-(4-methoxyphenyl)ethylidene)acetohydrazide (D1c)

2.3 (3H, s, methyl protons), 3.7 (3H, s, -OCH₃), 5.3 and 4.99 (2H; s; -N-CH₂-C=O), 6.9 (d, 2H, *J* = 8.8 Hz, phenyl protons), 7.1 (d; 1H; *J* = 9.6 Hz; pyridazinone H⁴), 7.5 (d, 2H, *J* = 8.8 Hz, phenyl

protons), 7.7 (d, 2H, *J* = 8.8 Hz, phenyl protons), 7.9 (d, 2H, *J* = 8.8 Hz, phenyl protons), 8.1 ppm (1H; d; *J* = 9.6 Hz; pyridazinone H⁵), 10.983 (1H; s; -NH-N). ¹³C-NMR (DMSO-*d*₆, 75 MHz), 12.55 (1C; -CH₃), 54.27 (1C; -N-CH₂-C=O), 55.38 (1C; -OCH₃), 113.84 (1C; =CH), 127.30 (1C; 4-methoxyphenyl C¹), 127.66 (4C; 4-methoxyphenyl C^{2,3,5,6}), 129.11 (5C; 4-chlorophenyl C^{1,2,3,5,6}), 130.05 (1C; 4-methoxyphenyl C⁴), 130.24 (1C; 4-chlorophenyl C⁴), 143.68 (1C; pyridazinone C⁵), 148.20 (1C; pyridazinone C⁶), 159.91 (1C; pyridazinone C⁴), 160.87 (1C; N-CH₂-C=O), 168.29 (1C; pyridazinone C³). C₂₁H₂₀N₄O₃Cl MS (ESI+) calculated: 411.1224 Found: *m/e* 411.1226 (M+H; % 100.0).

Table 1. Molecular structures, yields and melting points of D1a-f,2a-f



Comp.	R ₁	R ₂	R ₃	Yield (%)	M.P. (°C)
D1a	Cl	H	H	47	223
D1b	Cl	CH ₃	H	44	243
D1c	Cl	OCH ₃	H	40	232
D1d	Cl	OH	H	56	134
D1e	Cl	H	OCH ₃	61	210
D1f	Cl	Br	H	55	285
D2a	Br	H	H	43	231
D2b	Br	CH ₃	H	61	250
D2c	Br	OCH ₃	H	54	240
D2d	Br	OH	H	55	136
D2e	Br	H	OCH ₃	53	224
D2f	Br	Cl	H	50	289

2-(3-(4-chlorophenyl)-6-oxopyridazin-1(6H)-yl)-N'-(1-(4-hydroxyphenyl)ethylidene)acetohydrazide (DIId)

$^1\text{H-NMR}$ (DMSO- d_6 , 300 MHz), δ 2.3 (3H, s, methyl protons), 5.2 and 5.005 (2H; s; -N-CH₂-C=O), 6.9 (m, 2H, phenyl protons), 7.1 (d; 1H; 10 Hz; pyridazinone H⁴), 7.2 (m, 1H, phenyl protons), 7.5 (m, 1H, phenyl protons), 7.6 (d, 2H, J = 8 Hz, phenyl protons), 7.9 (d, 2H, J = 8.8 Hz, phenyl protons), 8.1 ppm (1H; d; J =10 Hz; pyridazinone H⁵), 11.3 (1H; s; -NH-N), 13 (1H; s; -OH proton). $^{13}\text{C-NMR}$ (DMSO- d_6 , 75 MHz), δ 13.736 (1C; -CH₃), 53.651 (1C; -N-CH₂-C=O), 117.233 (1C; =CH), 118.529 (1C; 4-hydroxyphenyl C¹), 119.199 (2C; 4-hydroxyphenyl C^{2,4}), 127.627 (2C; 4-hydroxyphenyl C^{3,5}), 128.458 (1C; 4-chlorophenyl C¹), 128.961 (1C; 4-chlorophenyl C⁴), 129.700 (2C; 4-chlorophenyl C^{3,5}), 131.186 (1C; 4-chlorophenyl C²), 133.015 (1C; 4-hydroxyphenyl C⁴), 134.272 (1C; 4-chlorophenyl C⁴), 142.685 (1C; pyridazinone C⁵), 155.845 (1C; pyridazinone C⁶), 158.481 (1C; pyridazinone C⁴), 158.961 (1C; N-CH₂-C=O), 163.785 (1C; pyridazinone C³). C₂₀H₁₈N₄O₃Cl MS (ESI+) calculated: 397.1067, Found: m/e 397.1053 (M+H; % 100.0).

2-(3-(4-chlorophenyl)-6-oxopyridazin-1(6H)-yl)-N'-(1-(2-methoxyphenyl)ethylidene)acetohydrazide (DIe)

$^1\text{H-NMR}$ (DMSO- d_6 , 300 MHz), δ 2.3 (3H, s, methyl protons), 3.8 (3H, s, -OCH₃), 5.19 and 4.99 (2H; s; -N-CH₂-C=O), 6.9 (m, 1H, phenyl protons), 7.1 (m; 1H phenyl proton and 1H pyridazinone H⁴), 7.1-6.9 (m, 2H, phenyl protons), 7.5 (d, 2H, J = 8.4 Hz, phenyl protons), 7.9 (d, 2H, J = 8.8 Hz, phenyl protons), 8.1 ppm (1H; d; J = 9.2 Hz; pyridazinone H⁵), 10.983 (1H; s; -NH-N). $^{13}\text{C-NMR}$ (DMSO- d_6 , 75

MHz), δ 16.38 (1C; -CH₃), 54.28 (1C; -N-CH₂-C=O), 55.42 (1C; -OCH₃), 111.06 (1C; =CH), 120.68 (2C; 2-methoxyphenyl C^{4,5}), 127.29 (1C; 2-methoxyphenyl C⁶), 129.08 (2C; 4-chlorophenyl C^{2,6}), 129.58 (1C; 4-chlorophenyl C¹), 130.23 (1C; 2-methoxyphenyl C¹), 130.34 (1C; 2-methoxyphenyl C³), 130.58 (2C; 4-chlorophenyl C^{3,5}), 133.18 (1C; 2-methoxyphenyl C²), 135.54 (1C; 4-chlorophenyl C⁴), 143.62 (1C; pyridazinone C⁵), 150.81 (1C; pyridazinone C⁶), 157.49 (1C; pyridazinone C⁴), 159.88 (1C; N-CH₂-C=O), 168.30 (1C; pyridazinone C³). C₂₁H₁₉N₄O₃Cl MS (ESI+) calculated: 411.1224, Found: m/e 411.1214 (M+H; % 100.0).

2-(3-(4-chlorophenyl)-6-oxopyridazin-1(6H)-yl)-N'-(1-(4-bromophenyl)ethylidene)acetohydrazide (DIIf)

$^1\text{H-NMR}$ (DMSO- d_6 , 300 MHz), δ 2.3 (3H, s, methyl protons), 5.3 and 5.001 (2H; s; -N-CH₂-C=O), 7.1 (d; 1H; 9.6 Hz; pyridazinone H⁴), 7.5 (m, 4H, phenyl protons), 7.7 (d, 2H, J = 8.4 Hz, phenyl protons), 7.9 (d, 2H, J = 8.8 Hz, phenyl protons), 8.1 ppm (1H; d; J = 10Hz; pyridazinone H⁵), 11 (1H; s; -NH-N). $^{13}\text{C-NMR}$ (DMSO- d_6 , 75 MHz), δ 13.525 (1C; -CH₃), 53.965 (1C; -N-CH₂-C=O), 122.707 (1C; =CH), 127.619 (1C; 4-bromophenyl C¹), 128.266 (2C; 4-bromophenyl C^{2,4}), 128.369 (2C; 4-bromophenyl C^{3,5}), 128.984 (1C; 4-chlorophenyl C¹), 129.677 (1C; 4-chlorophenyl C⁴), 131.068 (2C; 4-chlorophenyl C^{3,5}), 131.325 (1C; 4-chlorophenyl C²), 133.101 (1C; 4-bromophenyl C⁴), 134.229 (1C; 4-chlorophenyl C⁴), 137.082 (1C; pyridazinone C⁵), 142.507 (1C; pyridazinone C⁶), 147.681 (1C; pyridazinone C⁴), 159.069 (1C; N-CH₂-C=O), 168.687 (1C; pyridazinone C³). C₂₀H₁₆N₄O₂ClBr MS (ESI+) calculated: 459.0223, Found: m/e 459.0229 (M+H; % 100.0).

2-(3-(4-bromophenyl)-6-oxopyridazin-1(6H)-yl)-N'-(1-phenylethylidene)acetohydrazide (D2a)

¹H-NMR (DMSO-*d*₆, 300 MHz), δ 2.3 (3H, s, methyl protons), 5.3 and 5.015 (2H; s; -N-CH₂-C=O), 7.1 (1H; d; pyridazinone H⁵), 8.09 ppm (1H; d; pyridazinone H⁴), 7.8 (4H; m; phenyl protons), 7.4-7.6 (4H; m; phenyl protons), 10.986 (1H; s; -NH-N). ¹³C-NMR (DMSO-*d*₆, 75 MHz), δ 12.85 (1C; -CH₃), 54.27 (1C; -N-CH₂-C=O), 123.91 (1C; =CH), 126.21 (1C; phenyl C¹), 127.53 (2C; phenyl C^{2,6}), 128.49 (2C; phenyl C^{3,5}), 129.61 (1C; phenyl C⁴), 130.22 (1C; 4-bromophenyl C¹), 130.31 (2C; 4-bromophenyl C^{2,6}), 132.08 (2C; 4-bromophenyl C^{3,5}), 133.57 (1C; 4-bromophenyl C⁴), 137.59 (1C; pyridazinone C⁵), 143.69 (1C; pyridazinone C⁶), 148.84 (1C; pyridazinone C⁴), 159.92 (1C; N-CH₂-C=O), 168.76 (1C; pyridazinone C³). C₂₁H₁₉N₄O₂Br MS (ESI+) calculated: 425.0623, Found: *m/e* 425.0626 (M+H; % 100.0).

2-(3-(4-bromophenyl)-6-oxopyridazin-1(6H)-yl)-N'-(1-(*p*-tolyl)ethylidene)acetohydrazide (D2b)

¹H-NMR (DMSO-*d*₆, 300 MHz), δ 2.4 (3H, s, methyl protons), 2.2 (3H, s, methyl protons), 5.3 and 5.0 (2H; s; -N-CH₂-C=O), 7.1 (d; 1H; *J*= 9.6 Hz; pyridazinone H⁴), 7.2 (d, 2H, *J*= 8.4 Hz, phenyl protons), 7.7-7.6 (m, 4H, phenyl protons) ve 7.8 (d, 2H, *J*= 8.4 Hz, phenyl protons), 8.1 ppm (1H; d; *J*= 9.6 Hz; pyridazinone H⁵), 10.922 (1H; s; -NH-N). ¹³C-NMR (DMSO-*d*₆, 75 MHz), δ 12.65 (1C; -CH₃), 21.31 (1C; -CH₃), 54.28 (1C; -N-CH₂-C=O), 123.89 (1C; =CH), 126.14 (1C; 4-methylphenyl C¹), 127.55 (1C; 4-methylphenyl C⁴), 129.22 (2C; 4-methylphenyl C^{2,6}), 130.25 (2C; 4-methylphenyl C^{3,5}), 130.32 (1C; 4-bromophenyl C¹), 132.07 (2C; 4-bromophenyl C^{2,6}), 133.60 (2C; 4-bromophenyl C^{3,5}),

134.74 (1C; 4-bromophenyl C⁴), 139.86 (1C; pyridazinone C⁶), 143.72 (1C; pyridazinone C⁵), 148.60 (1C; pyridazinone C⁴), 159.91 (1C; N-CH₂-C=O), 168.41 (1C; pyridazinone C³). C₂₁H₁₉N₄O₂Br MS (ESI+) calculated: 439.0770, Found: *m/e* 439.0779 (M+H; % 100.0).

2-(3-(4-bromophenyl)-6-oxopyridazin-1(6H)-yl)-N'-(1-(4-methoxyphenyl)ethylidene)acetohydrazide (D2c)

¹H-NMR (DMSO-*d*₆, 300 MHz), δ 2.3 (3H, s, methyl protons), 3.7 (3H, s, -OCH₃), 5.3 and 4.99 (2H; s; -N-CH₂-C=O), 6.9 (d, 2H, *J*=8.8 Hz, phenyl protons), 7.1 (d; 1H; *J*=9.6 Hz; pyridazinone H⁴), 7.6 (d, 2H, *J*= 8.4 Hz, phenyl protons), 7.7 (d, 2H, *J*= 8.4 Hz, phenyl protons), 7.8 (d, 2H, 2H, *J*= 8.4 Hz, phenyl protons), 8.1 ppm (1H; d; *J*= 9.6 Hz; pyridazinone H⁵), 10.983 (1H; s; -NH-N). ¹³C-NMR (DMSO-*d*₆, 75 MHz), δ 12.55 (1C; -CH₃), 54.29 (1C; -N-CH₂-C=O), 55.39 (1C; -OCH₃), 113.84 (1C; =CH), 123.88 (1C; 4-methoxyphenyl C¹), 127.55 (4C; 4-methoxyphenyl C^{2,3,5,6}), 127.66 (4C; 4-bromophenyl C^{2,3,5,6}), 130.05 (1C; 4-bromophenyl C¹), 130.25 (1C; 4-methoxyphenyl C⁴), 130.32 (1C; 4-bromophenyl C⁴), 132.07 (1C; pyridazinone C⁵), 133.61 (1C; pyridazinone C⁶), 159.91 (1C; pyridazinone C⁴), 160.87 (1C; N-CH₂-C=O), 168.28 (1C; pyridazinone C³). C₂₁H₁₉N₄O₃Br MS (ESI+) calculated: 455.0719, Found: *m/e* 455.0682 (M+H; % 100.0).

2-(3-(4-bromophenyl)-6-oxopyridazin-1(6H)-yl)-N'-(1-(4-hydroxyphenyl)ethylidene)acetohydrazide (D2d)

¹H-NMR (DMSO-*d*₆, 300 MHz), δ 2.3 (3H, s, methyl protons), 5.213 and 5.053 (2H; s; -N-CH₂-C=O), 6.9 (m, 2H, phenyl protons), 7.1 (d; 1H; *J*=10 Hz;

pyridazinone H⁴), 7.3 (m, 1H, phenyl protons), 7.6 (m, 1H, phenyl protons), 7.7 (d, 2H, *J*=8.4 Hz, phenyl protons), 7.8 (d, 2H, *J*= 8.4 Hz, phenyl protons), 8.1 ppm (1H; d; *J*=10 Hz; pyridazinone H⁵), 11.4(1H; s; -NH-N), 13 (1H; s; -OH proton). ¹³C-NMR (DMSO-*d*₆, 75 MHz), δ 13.743 (1C; -CH₃), 53.657 (1C; -N-CH₂-C=O), 117.238 (1C; =CH), 118.533 (1C; 4-hydroxyphenyl C¹), 119.200 (2C; 4-hydroxyphenyl C^{2,4}), 123.021 (2C; 4-hydroxyphenyl C^{3,5}), 127.881 (1C; 4-chlorophenyl C¹), 128.458 (1C; 4-chlorophenyl C⁴), 129.702 (2C; 4-chlorophenyl C^{3,5}), 131.171 (1C; 4-chlorophenyl C²), 131.882 (1C; 4-hydroxyphenyl C⁴), 133.376 (1C; 4-chlorophenyl C⁴), 142.763 (1C; pyridazinone C⁵), 155.856 (1C; pyridazinone C⁶), 158.479 (1C; pyridazinone C⁴), 158.966 (1C; N-CH₂-C=O), 163.775 (1C; pyridazinone C³). C₂₀H₁₇N₄O₃Br MS (ESI+) calculated: 441.0562, Found: *m/e* 441.0574 (M+H; % 100.0).

2-(3-(4-bromophenyl)-6-oxopyridazin-1(6H)-yl)-N'-(1-(2-methoxyphenyl)ethylidene)acetohydrazide (D2e)

¹H-NMR (DMSO-*d*₆, 300 MHz), δ 2.3 (3H, s, methyl protons), 3.8 (3H, s, -OCH₃), 5.19 and 4.99 (2H; s; -N-CH₂-C=O), 6.9 (m, 1H, phenyl protons), 7.1 (m; 1H phenyl protons and 1H pyridazinon H⁴), 7.3-7.2 (m, 2H, phenyl protons), 7.6 (d, 2H, *J*=8.8 Hz, phenyl protons), 7.8 (d, 2H, *J*= 8.8 Hz, phenyl protons), 8.1 ppm (1H; d; *J*= 10 Hz; pyridazinone H⁵), 10.983 (1H; s; -NH-N). ¹³C-NMR (DMSO-*d*₆, 75 MHz), δ 16.44 (1C; -CH₃), 54.29 (1C; -N-CH₂-C=O), 55.42 (1C; -OCH₃), 111.06 (1C; =CH), 120.687 (4C; 2-methoxyphenyl C^{3,4,5,6}), 127.54 (2C; 4-bromophenyl C^{2,3,5,6}), 129.59 (1C; 4-bromophenyl C¹), 130.22 (1C; 2-methoxyphenyl C¹), 130.56 (1C;

2-methoxyphenyl C²), 132.03(1C; 4-bromophenyl C⁴), 143.63 (1C; pyridazinone C⁵), 150.96 (1C; pyridazinone C⁶), 157.48 (1C; pyridazinone C⁴), 159.89 (1C; N-CH₂-C=O), 168.41 (1C; pyridazinone C³). C₂₁H₁₉N₄O₃Br MS (ESI+) calculated: 455.0719, Found: *m/e* 459.0700 (M+H; % 100.0).

2-(3-(4-bromophenyl)-6-oxopyridazin-1(6H)-yl)-N'-(1-(4-chlorophenyl)ethylidene)acetohydrazide (D2f)

¹H-NMR (DMSO-*d*₆, 300 MHz), δ 2.3 (3H, s, methyl protons), 5.3 and 5.01 (2H; s; -N-CH₂-C=O), 7.1 (d; 1H; *J*=10 Hz; pyridazinone H⁴), 7.45 (d, 2H, *J*=8.8 Hz phenyl protons), 7.65 (d, 2H, *J*=8.8 Hz, phenyl protons), 7.8 (m, 4H, phenyl protons), 8.1 ppm (1H; d; *J*=9.6 Hz; pyridazinone H⁵), 11.02 (1H; s; -NH-N). ¹³C-NMR (DMSO-*d*₆, 75 MHz), δ 13.404 (1C; -CH₃), 53.754 (1C; -N-CH₂-C=O), 122.797 (1C; =CH), 127.708 (1C; 4-bromophenyl C¹), 127.817 (2C; 4-bromophenyl C^{2,4}), 128.221 (2C; 4-bromophenyl C^{3,5}), 129.510 (1C; 4-chlorophenyl C¹), 130.792 (2C; 4-chlorophenyl C^{3,5}), 131.722 (2C; 4-chlorophenyl C^{2,4}), 133.376 (1C; 4-bromophenyl C⁴), 133.793 (1C; 4-chlorophenyl C⁴), 136.634 (1C; pyridazinone C⁵), 142.449 (1C; pyridazinone C⁶), 147.502 (1C; pyridazinone C⁴), 158.915 (1C; N-CH₂-C=O), 168.449 (1C; pyridazinone C³). C₂₀H₁₆N₄O₂ClBr MS (ESI+) calculated: 459.0228, Found: *m/e* 459.0244 (M+H; % 100.0).

3.2. Anticholinesterase Activity

The *in vitro* inhibition of AChE and BChE for the synthesized title compounds was determined by the method of Ellman et al. (1961). The activity results are given in Table 2. The vast majority of compounds have BChE inhibitory effects., except for compounds **D_{1f}** and **D_{2f}**, the others also showed an

AChE inhibitory effect. The compounds showed a higher inhibitory effect against BChE than against AChE. Compound **D_{2a}** showed almost the same efficacy as the reference drug galantamine, while compounds **D_{1a}** and **D_{2e}** showed higher activity than galantamine. Compound **D_{2e}** bearing bromophenyl and 2-methoxyphenyl rings showed to have the best BChE inhibitor effect, 57.42 ± 3.69 % ($IC_{50} = 38.45 \pm 2.44$ μ M) inhibition of BChE (Table 2).

3.3. Molecular Docking / MD Simulations Studies

In order to define the binding modes between the ligand and the receptor, docking studies were carried with the AChE (PDB ID: 4EY7) and BChE (PDB ID: 4BDS) proteins (Alagöz et al. 2019). The docking scores of synthesized compounds, tacrin (native ligand) and galantamine (reference molecule) are given in Table 3.

For the validation studies of the molecular modeling study, the tacrine molecule in the protein crystal structure was removed, minimized, redocked and the RMSD 0.124 Å was calculated. Docking scores of the compounds in BChE inhibition were found between -4.530 and -7.805 kcal/mol. The docking scores of compound **D_{2e}** which had the best BChE inhibition, tacrine and galantamine, were calculated as -7,805, -7,188, -6,998 kcal/mol, respectively. Compound **D_{2e}** made hydrogen bonds with GLY115, GLY116, GLY117, SER198, ALA199, SER287 located in the active site of the enzyme. It also interacted hydrophobically with TRP82, TYR128, ALA199, TYR332; Polar interaction with SER198, SER287, HIS438; It has pi-pi stacking interaction with TRP82 and HIS438. Tacrine, on the other hand, hydrogen bonded with HIS438, hydrophobic

interaction with TRP82, PHE329, TRP430, 440, and ionic interaction with ASP70 (Figure 3).

After molecular docking studies, molecular dynamics simulation studies were performed with compound **D_{2e}** and tacrine with the best docking score. MD simulation studies were started from the conformation of the compounds with the lowest binding energy. In simulation studies, the interaction of compound **D_{2e}** and tacrine with protein was evaluated for 50 ns. (Figure 4, Figure 5).

When the specific interactions of Tacrine and **D_{2e}** with the protein for 50ns were examined, it was observed that especially TRP82, HIS438 made multiple contacts and were therefore represented in dark orange color.

4. Discussion

4.1. Synthesis

In this study, as a continuation of our previous studies on benzalhydrazone derivatives, it was aimed to synthesize some new hydrazone derivatives as potential anticholinesterase compounds with better binding affinity and then to evaluate their anticholinesterase activity. In the benzalhydrazone derivatives, from nonsubstituted to trisubstituted as acetophenone groups bearing methyl, methoxy, chloro and bromo were prepared as different substituents.

Synthesis of the compounds was initiated by obtaining 6-chloro/bromophenyl-3(2H)pyridazinone. A very useful and easy to use method was tested for the synthesis of compound these compounds (**A1, A2**), which Schmidt and Druey developed in 1954 for the synthesis of pyridazinone compounds (

Schmidt & Druey, 1954). The reaction is based on the formation of 3(2*H*)-pyridazinone derivatives by condensation of 1,2-dicarbonyl compound with monosubstituted or unsubstituted hydrazine and the carboxyl derivative containing active methylene group. Dicarbonyl compounds include 1,2-diketones, α -ketoacids or glyoxal and esters; malonic acid, acetoacetic acid, cyanoacetic acid, benzoyl acetic acid or hippuric acid esters are used as a reactive group of α -methylene (Lapinski et al., 1992). In this study, glyoxalic acid was used as 1,2-dicarbonyl compound. Glyoxalic acid and acetophenone derivatives were heated with hydrazine hydrate in acidic medium to give 3(2*H*)-pyridazinone derivative

A1, A2 compounds (Katritzky & Lagowski, 1963). Ethyl 6-substituted-3(2*H*)-pyridazinone-2-ylacetate derivatives (**B1, B2**) were obtained by the reaction of **A1, A2** with ethyl bromoacetate in the presence of K_2CO_3 in acetone (Özdemir et al., 2017; Bozbey et al., 2020). Then, 6-substituted-3(2*H*)-pyridazinone-2-ylacetohydrazide derivatives (**C1, C2**) were synthesized by the condensation reaction of **B1, B2** with hydrazine hydrate (99%) (Özdemir et al., 2017; Bozbey et al., 2020). Ultimately, the title compounds bearing benzalhydrazone structure were obtained by the reaction of **C1, C2** with substituted/nonsubstituted acetophenone.

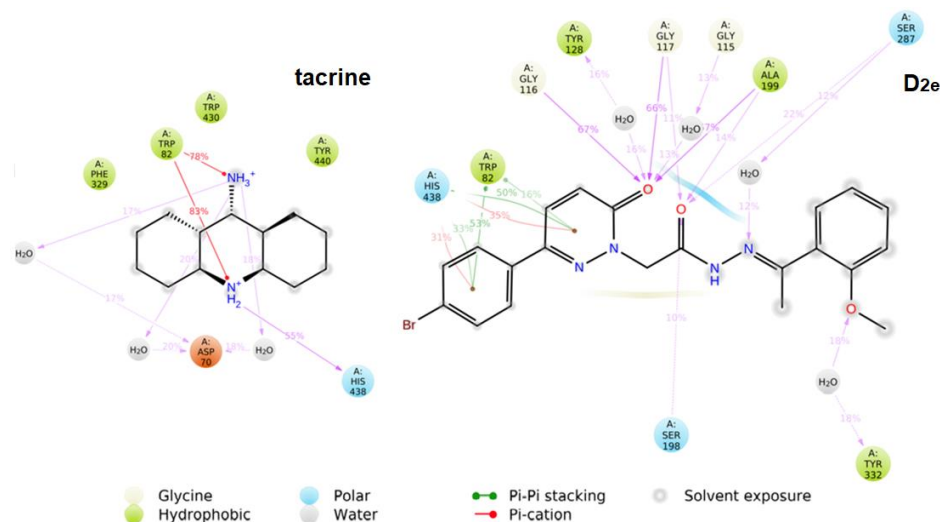


Figure 3. 2D Interaction of tacrine and compound D2e with the active site of BChE

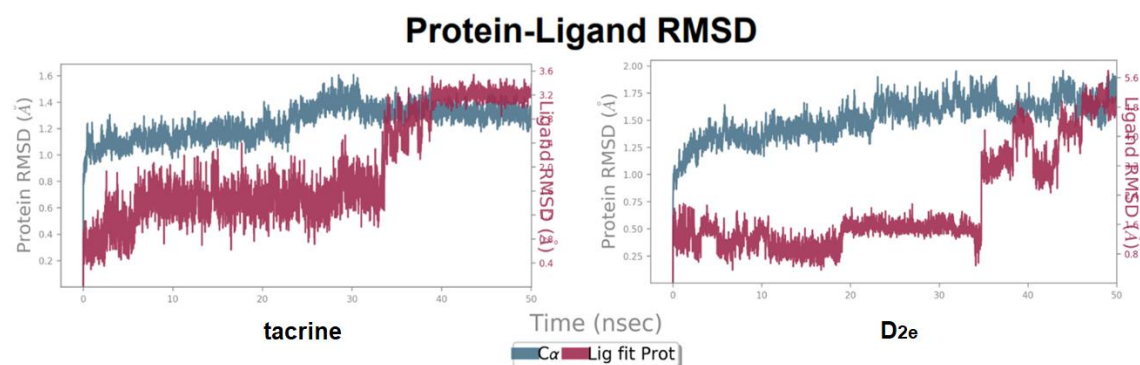


Figure 4. The Root Mean Square Deviations (RMSD) plots. RMSDs for tacrine and compound 2D.

Table 2. AChE and BChE inhibition values (%) of the title compounds at 100 μ M

	AChE inhibition (Inhibition \pm SD ^a) 100 μ M ^b	BChE inhibition (Inhibition \pm SD ^a) 100 μ M ^b
D _{1a}	7.80 \pm 0.13	39.97 \pm 4.06
D _{1b}	8.59 \pm 2.93	21.80 \pm 3.23
D _{1c}	11.15 \pm 3.15	22.91 \pm 4.78
D _{1d}	12.82 \pm 3.48	19.48 \pm 2.71
D _{1e}	12.89 \pm 1.55	21.87 \pm 3.33
D _{1f}	- ^c	20.04 \pm 1.97
D _{2a}	6.59 \pm 0.39	37.86 \pm 3.43
D _{2b}	11.76 \pm 3.95	13.98 \pm 3.92
D _{2c}	12.62 \pm 2.16	15.20 \pm 3.71
D _{2d}	34.23 \pm 3.23	34.02 \pm 5.83
D _{2e}	23.27 \pm 4.19	57.42 \pm 3.69*
D _{2f}	- ^c	19.48 \pm 1.77*
Galantamine	86.05 \pm 2.12	37.91 \pm 1.22

^a Standard deviation (n=4), ^b Final concentration, ^c did not show inhibitory activity, * (concentration 50 μ M)

4.2. Anticholinesterase Activity

In our previous studies, 6-(substituted phenyl)-3(2H)-pyridazinone derivatives with cholinesterase inhibitory effect were synthesized and published. The activities of these derivatives (0.25 mM and 0.50 mM concentrations) were evaluated against galantamine [19]. Again, 6-(substituted phenyl)-3(2H)-pyridazinone-2-acetyl-2-(substituted-acetophenone) hydrazone derivatives with a different structure were synthesized by our study group and they were found to have high cholinesterase inhibitory activity at 0.05 mM, 0.1 and 0.2 mM concentrations. determined (Heo et al., 2004). In order to contribute to the

structure-activity studies of these two studies, the new derivatives with the same skeleton (3(2H)-pyridazinone) do not have the piperazine ring in the 6th position of the pyridazinone ring.

The BChE inhibition effects of the compounds were evaluated using galantamine as the reference compound. The substitution of Cl or Br atoms to the phenyl ring attached to the pyridazinone ring did not cause a significant change in the activity. Derivatives without substituents in the other phenyl ring attached to the hydrazone moiety in the structure of the compounds showed high BChE inhibition activity. With the addition of methyl, methoxy and hydroxyl

substituents to this second phenyl ring, changes in activity were observed. Very high activity was observed in the **D2e** compound, which has a Br substituent in the phenyl ring attached to pyridazinone and a methoxy substituent in the second position of the other phenyl ring. This is thought to be because the conformation of the compound changes, making stronger H bonds with significant residues in the active site of the protein. These interactions have been supported by molecular docking and MD studies.

4.3. Molecular Docking/MD Simulations

Studies

When the docking results were examined, compounds **D1c**, **D2c** showing low BChE inhibition, were observed to be the compounds interacted hydrophobically and polarly with various residues in the active site but did not interact with TRP82 and HIS438. According to these data, it was found that interaction with TRP 82 and HIS 438 in the active site of the enzyme is very important for BChE inhibition.

MD trajectories analyzes of ligands are shown in Figure 5. Changes of the order of 1-3 Å are perfectly acceptable for small, globular proteins. According to the analysis results, it is seen that the root mean square deviations (RMSD) values of the alpha carbons (C α) of the protein (4BDS) vary between 0.8 and 1.75 Å. The RMSD value of Tacrine is between 0.2 - 3.3 Å for 50 ns, the RMSD value of D2e is between 0.25 - 0.58 Å.

Table 3: Docking scores of compounds

Compounds	BChE inhibition	AChE inhibition
D1a	-6,438	-4,218
D1b	-5,904	-4,890
D1c	-5,836	-4,305
D1d	-4,530	-4,230
D1e	-5,682	-4,462
D1f	-5,366	-4,697
D2a	-6,949	-4,096
D2b	-4,925	-3,918
D2c	-4,733	-6,035
D2d	-5,826	-4,346
D2e	-7,805	-6,321
D2f	-5,818	-5,204
Galantamine	-6,998	-7,808
Tacrine	-7,188	-6,419

Conclusions

In order to develop new choline esterase inhibitor compounds, 12 new 2,6-disubstituted-3-(2*H*)-pyridazinone derivatives were designed and synthesized. With this study, which is a continuation of our previous studies, the structure-activity relationship of compounds with 3-(2*H*)-pyridazinone skeleton was developed. Although the AChE inhibitory effects of these new compounds were quite low, significant BChE inhibitory activities were detected. The selective BChE inhibitory activities of the compounds were also supported by in silico studies.

Conflicts of interest

The authors confirm that this article content has no conflict of interest.

Acknowledgement

This work was supported by Research Foundation of Gazi University (02/2017-22).

References

- Ahmed, E. M. , Hassan, M. S. , El-Malah, A. A., Kassab, A. E. (2020). New pyridazine derivatives as selective COX-2 inhibitors and potential anti-inflammatory agents; design, synthesis and biological evaluation., *Bioorganic Chemistry*, 95, 103497. <https://doi.org/10.1016/j.bioorg.2019.103497>
- Alagöz, M. A. , Özdemir, Z., Özçelik, A. B. (2019). Molecular Modelling Studies of Pyridazinone Derivatives as Antibutrylcholinesterases. *International Journal of Pharmacy and Chemistry*, 5(3), 26-30. <https://doi.org/10.11648/j.ijpc.20190503.11>
- Anand, P. & P. Singh,P. (2013). A review on cholinesterase inhibitors for Alzheimer's disease. *Archives of Pharmacal Research*, 36, 375-399. <https://doi.org/10.1007/s12272-013-0036-3>
- Banerjee, P. S. (2011). Various Biological Activities of Pyridazinone Ring Derivatives. *Asian Journal of Chemistry*, 23, 1905-1910.
- Bozbey, İ. , Özdemir, Z., Uslu, H. , Özçelik, A. B. , Şenol, F. S., Orhan-Erdoğan, İ., Uysal, M. (2020). A Series of New Hydrazone Derivatives: Synthesis, Molecular Docking and Anticholinesterase Activity Studies. *Mini-Reviews in Medicinal Chemistry*, 20(11), 1042-1060. <https://doi.org/10.2174/1389557519666191010154444>
- Çeçen,M., Oh, J. M. , Özdemir, Z., Büyüktuncel, S. E. . Uysal, M., Abdelgawad, M. A. ,. Musa,A., Gambacorta, N., Nicolotti, O., Mathew, B. , Kim H. (2020). Design, Synthesis, and Biological Evaluation of Pyridazinones Containing the (2-Fluorophenyl) Piperazine Moiety as Selective MAO-B Inhibitors. *Molecules*, 25(22), 5371. <https://doi.org/10.3390/molecules25225371>
- Chatonnet, A. & Lockridge, O. (1989). Comparison of butyrylcholinesterase and acetylcholinesterase. *Biochemical Journal*, 260(3), 625-634. <https://doi.org/10.1042/bj2600625>
- Ciftci, O. , Özdemir, Z., Acar, C. , Sözen, M. , Basak-Türkmen, N., Ayhan, I., Gözükara, H. (2018). The Novel Synthesized Pyridazinone Derivates had the Antiproliferative and Apoptotic Effects in SHSY5Y and HEP3B Cancer Cell Line. *Letters in Organic Chemistry*, 15(4), 323-331. <https://doi.org/10.2174/1570178614666170707154210>
- Costas-Lago, M. C. , Besada, P. , Rodriguez-Enriquez, F., Viña, D., Vilar, S., Uriarte, E., Borges, F. , Terán, C. (2017).Synthesis and structure-activity relationship study of novel 3-heteroarylcoumarins based on pyridazine scaffold as selective MAO-B inhibitors. *European Journal of Medicinal Chemistry*., 139, 1-11. <https://doi.org/10.1016/j.ejmech.2017.07.045>
- Dvir, H., Silman, I., Harel, M., Rosenberry, T. L. , Sussmana, J. L. (2010). Acetylcholinesterase: from 3D structure to function. *Chemico-Biological Interactions*, 187, 10-22. <https://doi.org/10.1016/j.cbi.2010.01.042>
- Ellman, G. L., Courtney, K. D., Andres Jr, V., & Featherstone, R. M. (1961). A new and rapid colorimetric determination of acetylcholinesterase activity. *Biochemical pharmacology*, 7(2), 88-95. [https://doi.org/10.1016/0006-2952\(61\)90145-9](https://doi.org/10.1016/0006-2952(61)90145-9)
- Hampel, H., Mesulam, M. M., Cuello, A. C., Farlow, M. R., Giacobini, E., Grossberg, G. T., Khachaturian., Vergallo, A. S. A, Cavedo,E., Snyder, P. J., Khachaturian, Z. S. (2018). The cholinergic system in the pathophysiology and treatment of Alzheimer's disease. *Brain*, 141(7), 1917-1933. <https://doi.org/10.1093/brain/awy132>
- Heo, H. J. , Kim, M. J. , Lee, J. M. , Choi, S. J. , Cho, H. Y. , Hong, B. , Kim, H. K. , Kim, E., Shin, D. H.. (2004). Naringenin from Citrus junos has an inhibitory effect on acetylcholinesterase and a mitigating effect on amnesia. *Dementia and Geriatric Cognitive Disorders*, 17, 151-157. <https://doi.org/10.1159/000076349>
- Katritzky, A. R. & Lagowski, J. M. (1963). Prototropic Tautomerism of Heteroaromatic Compounds: I. General Discussion and Methods of Study. *Advances in Heterocyclic Chemistry*, 1, 311-338. [https://doi.org/10.1016/S0065-2725\(08\)60528-0](https://doi.org/10.1016/S0065-2725(08)60528-0)
- Kilic, B., Gulcan, H. O. , Aksakal, F. (2018). Design and synthesis of some new carboxamide and propanamide derivatives bearing phenylpyridazine as a core ring and the investigation of their inhibitory potential on in-vitro acetylcholinesterase and butyrylcholinesterase. *Bioorganic Chemistry*, 79, 235-249. <https://doi.org/10.1016/j.bioorg.2018.05.006>
- Lapinski, L., Nowak, M. J. , Fulara, J. , Les', A., Adamowicz, L. (1992). Relation between structure and tautomerism in diazinones and diazinethlones. An experimental matrix isolation and theoretical ab initio study. *The Journal of Physical Chemistry*, 96, 6250-6254.
- Orhan, S., Aslan, M.İ, Kartal, B.İ Şener, K. H. C. Başer, (2008). Inhibitory effect of Turkish Rosmarinus officinalis L. On acetylcholinesterase and butyrylcholinesterase enzymes. *Food Chemistry*, 108663-668. <https://doi.org/10.1016/j.foodchem.2007.11.023>
- Özçelik, A. B., Özdemir, Z., Sari, S. , Utku, S. , Uysal, M. (2019). A New Series of Pyridazinone Derivatives as Cholinesterases Inhibitors: Synthesis, In Vitro Activity and Molecular Modeling Studies. *Pharmacological Reports*, 71(6), 1253-1263. <https://doi.org/10.1016/j.pharep.2019.07.006>
- Özdemir, Z. , Yılmaz, H., Sari, S., Karakurt, A., Şenol, F. S., Uysal, M. (2017). Design, synthesis, and molecular modeling of new 3(2H)-pyridazinone derivatives as acetylcholinesterase/butyrylcholinesterase inhibitors. *Medicinal Chemistry Research*, 26, 2293-2308. <https://doi.org/10.1007/s00044-017-1930-x>

- Özdemir, Z., Başak-Türkmen, N., Ayhan, İ., Çiftçi, O., M. Uysal, M. (2019). Synthesis of New 6-[4-(2-Fluorophenylpiperazine-1-yl)]-3(2H)-pyridazinone-2-acetyl-2-(substitutedbenzal)hydrazone Derivatives and Evaluation of Their Cytotoxic Effects in Liver and Colon Cancer Cell Line. *Pharmaceutical Chemistry Journal*, 52;11, 952-959. <https://doi.org/10.1007/s11094-019-01927-y>
- Özdemir, Z., Alagöz, M. A. (2019). Anticholinesterases (Eds: I. J. Al-Zwaini, A. AL-Mayahi), Selected Topics in Myasthenia Gravis. 1st edition. London: *Intech Open*, 69-78. <https://doi.org/10.2174/0929867328666210203204710>
- Özten, Ö., Zengin Kurt, B., Sönmez, F., Doğan, B., Durdagi, S. (2021). Synthesis, molecular docking and molecular dynamics studies of novel tacrine-carbamate derivatives as potent cholinesterase inhibitors. *Bioorganic Chemistry*, 115105225. <https://doi.org/10.1016/j.bioorg.2021.105225>
- Rathish, I. G., Javed, K., Bano, S., Ahmad, S., Alam, M. S., Pillai, K. K. (2009). Synthesis and blood glucose lowering effect of novel pyridazinone substituted benzenesulfonylurea derivatives. *European Journal of Medicinal Chemistry*, 44, 2673-2678. <https://doi.org/10.1016/j.ejmech.2008.12.013>
- Roth, G. J., Heckel, A., Kley, J. T. (2015). Design, synthesis and evaluation of MCH receptor 1 antagonists-Part II: optimization of pyridazines toward reduced phospholipidosis and hERG inhibition. *Bioorganic & Medicinal Chemistry Letters*, 25, 3270-3274. <https://doi.org/10.1016/j.bmcl.2015.05.074>
- Sabt, A., Eldehna, W. M., Al-Warhi, T., Alotaibi, O. J., Elaasser, M. M., Suliman, H., Abdel-Aziz, H. A. (2020). Discovery of 3,6- disubstituted pyridazines as a novel class of anticancer agents targeting cyclin-dependent kinase 2: synthesis, biological evaluation and in silico insights *Journal of Enzyme Inhibition and Medicinal Chemistry*, 35(1), 1616-1630. <https://doi.org/10.1080/14756366.2020.1806259>
- Sameem, B., Saeedi, M., Mahdavi, M., Shafiee, A. (2018). A review on tacrine-based scaffolds as multi-target drugs (MTDLs) for Alzheimer's disease. *European Journal of Medicinal Chemistry*, 128(10), 332-345. <https://doi.org/10.1016/j.ejmech.2016.10.060>
- Schmidt, P., Druey, J. (1954). Heilmittelchemische Studien in der heterocyclischen Reihe. 10. Mitteilung. Pyridazine VII. Zur neuen Pyridazin-Synthese. Methylpyridazine. *Helvetica Chimica Acta*. 37(5), 1467-1471. <https://doi.org/10.1002/HLCA.19540370514>
- Tan, O. U., Ozadali, K., Yogeewari, P. (2012). Synthesis and antimycobacterial activities of some new N-acylhydrazone and thiosemicarbazide derivatives of 6-methyl-4,5-dihydropyridazin-3(2H)-one. *Medicinal Chemistry Research*, 21, 2388-2394. <https://doi.org/10.1007/s00044-011-9770-6>
- Türkeş, C., Akocak, S., Işık, M., Lolak, N., Taslimi, P., Durgun, M., Gülçin, İ., Budak, Y., Beydemir, Ş. (2021). Novel inhibitors with sulfamethazine backbone: synthesis and biological study of multi-target cholinesterases and α -glucosidase inhibitors. *Journal of Biomolecular Structure and Dynamics*, 40(5), 1-13. <https://doi.org/10.1080/07391102.2021.1916599>
- Utku, I., Gökçe, M., Aslan, G., Bayram, G., Ülger, M., Emekdaş, G., Şahin, M. F. (2011). Synthesis and *in vitro* antimycobacterial activities of novel 6-substituted-3(2H)-pyridazinone-2-acetyl-2-(substituted/nonsubstituted acetophenone) hydrazine. *Arzneimittelforschung*, 61(1), 1-7. <https://doi.org/10.3906/kim-1009-63>
- Utku, S., Gökçe, M., Orhan, İ., Şahin, M. F. (2011). Synthesis of novel 6-substituted-3(2H)-pyridazinone-2-acetyl-2-(substituted/-nonsubstituted benzal)hydrazone derivatives and acetylcholinesterase and butyrylcholinesterase inhibitory activities *in vitro*. *Journal of Chemistry*, 829(35), 331-339. <https://doi.org/10.1055/s-0031-1296161>
- Yamali, C., Ozan, G. H., Kahya, B., Çobanoğlu, S., Şüküroğlu, M. K., Doğruer, D. S. (2015). Synthesis of some 3(2H)-pyridazinone and 1(2H)-phthalazinone derivatives incorporating aminothiazole moiety and investigation of their antioxidant, acetylcholinesterase, and butyrylcholinesterase inhibitory activities. *Medicinal Chemistry Research*, 24, 1210-1217. <https://doi.org/10.1007/s00044-014-1205-8>